Available online at www.sciencedirect.com
SCIENCE DIRECT
Polymer 47 (2006) 6042–6047
polymer
www.elsevier.com/locate/polymer

Polymer Communication

Mechanism of dc electrical conduction and human endothelial cell proliferation in polypyrrole/sodium nitrate membrane

Ramadhar Singh [a,*], Jitendra Kumar [a], Amarjeet Kaur [b], K.L. Yadav [c], R. Bhattacharyya [a], Ejaz Hussain [d], Sher Ali [d]

[a] *National Physical Laboratory, Polymeric Devices Group, Dr. K.S. Krishnan Marg, New Delhi-110012, India*
[b] *Department of Physics and Astrophysics, University of Delhi, New Delhi-110007, India*
[c] *Department of Physics, Indian Institute of Technology, Roorkee-226707, India*
[d] *National Institute of Immunology, New Delhi-110067, India*

Received 22 September 2005; received in revised form 21 June 2006; accepted 25 June 2006
Available online 12 July 2006

Abstract

We have synthesized and characterized polypyrrole/sodium nitrate (PPY/$NaNO_3$) membranes that can be used as substrate to support human endothelial cell proliferation. Furthermore, the mechanism of electrical transport in this system is examined in the temperature range 13–300 K before it could be used as a substrate for human endothelial cell growth. The polymer membrane reported here is biocompatible in nature and therefore, it is envisaged to be highly useful for the growth and development of bioartificial organs. This has a great potential in the context of medical biotechnology.

Keywords: PPY/$NaNO_3$ membrane; dc Electrical conduction; Human endothelial cell proliferation

1. Introduction

The electronic properties of conjugated polymers have acquired a growing importance in many areas of modern chemistry, biotechnology and physics of condensed matter. There exist numerous applications [1,2] of conjugated polymers which depend upon the tailoring of its appropriate properties for a particular application. In view of the wide-ranging applications, a considerable attention has been paid to the polypyrrole family of polymers, prepared by electrochemical and chemical oxidation method [2]. Polypyrrole (PPY) has been extensively investigated [2,3] because it is relatively stable, simple to produce, has good mechanical strength and high conductivity. It can be synthesized to contain a variety of (poly)anions. Previous studies [4–8] have identified PPY as a novel substrate for the support of mammalian cell growth indicating thereby a potential utility of this polymer as a ''Smart Biomaterial''. The electrostatic interaction between the negatively charged deoxyribonucleic acid (DNA) and the positively charged PPY surfaces has been investigated [9]. Recently, a conductive polypyrrole modified microelectrode for selective amperometric detection of nitrate in a flow injection system has been developed [10]. It is evident from literature [7,11] that polypyrrole composites can be used to support nerve cell growth, neurite extension, coating of vascular stents and other prostheses. Of special interest, is the use of this polymer in tissue engineering [12]. The design of a wide array of surgical implants, artificial organs and wound closure devices is critically dependent on available biomaterials [4–8]. This has evoked our interest to synthesize and characterize polypyrrole/sodium nitrate (PPY/$NaNO_3$) membranes for its use as substrates to support human endothelial cell proliferation. In spite of the extensive studies [2,3,13–15] on conducting polypyrrole and its composites to

* Corresponding author. Tel.: +91 11 2574 2610x2303; fax: +91 11 2572 6938.
E-mail address: ramadhar@mail.nplindia.ernet.in (R. Singh).

0032-3861/$ - see front matter © 2006 Elsevier Ltd. All rights reserved.
doi:10.1016/j.polymer.2006.06.057

improve the material quality and to understand the physical processes in this system, no report about the electrical transport mechanism of PPY/$NaNO_3$ membrane and human endothelial cell proliferation exists in the literature. We report here the mechanism of electrical transport in PPY/$NaNO_3$ membrane to ascertain that the same may be used as a substrate for human endothelial cell growth. To this end, the dc conductivity of this membrane has been investigated in the temperature range 13–300 K and the biomedical application of the membrane is highlighted.

2. Experimental

Electrochemical polymerization of PPY/$NaNO_3$ [$PPY^+(NO_3^-)$] membranes was carried out under constant current of 0.5 mA/cm^2 for 25 min in a single compartment cell on 2.5×4 cm^2 platinum plates as electrodes at 273 K in an inert atmosphere. Reagent grade pyrrole (M/S Fluka Chemie A. G.) was doubly distilled before use. The concentration of pyrrole and the supporting electrolyte $NaNO_3$ (BDH, E. Merck, India) was 0.1 M and 0.8 M, respectively. The synthesis of the membrane was confirmed by obtaining Fourier transform infrared (FT-IR) spectrum, recorded on a Perkin–Elmer Model-2000 Opticaspectrometer. Atomic force microscopic (AFM) analysis was carried out using a Digital Nanoscope II scanning probe microscope in contact mode to determine the surface roughness and homogeneity of the $PPY^+(NO_3^-)$ film. For the surface morphology investigation, scanning electron micrograph (SEM) of the samples was obtained using a scanning electron microscope Model LEO S440. Four dots of gold having 2 mm diameter were vacuum evaporated on the samples for the measurement of dc conductivity. The dc conductivity was measured in the temperature range 13–300 K by four probe technique in a Cryocooler (APD Model Displex DE 202) fitted with a Temperature Controller model 9650 (Scientific Instruments) by using Keithley's 224 Constant current source and 181 Nanovoltmeter.

Human endothelial cell line (ECV304) obtained from American type culture collection (ATCC, Rockville, MD) was used in this study. The cell lines were maintained in RPMI (Sigma) supplemented with 10% fetal calf serum (FCS) and 1% antibiotic (penicillin/streptomycin) in disposable culture flasks (T25 and T75) at 310 K in 5% CO_2. Cells were passaged at 4 day intervals. Stock cells were trypsinized and suspended at 10^6 cells/ml in the medium. Autoclaved polypyrrole/sodium nitrate composite membranes were placed in six well culture plates and then 1 ml of the stock cell culture (containing 1×10^6 cells) and 4 ml of media were added on top of these membranes. Cells were allowed to grow for 72–96 h at 310 K in a CO_2 incubator. As the membranes were opaque, the adhesion and growth of the cells were observed through a fluorescent microscope by placing the membrane on a slide and adding 100 μl of fluorescent dye (fluorochrome) on the surface of the membrane. Photographs were taken on Nikon Microscope Alphaphot-YS fitted with automatic photo micrographic camera system FX 35 WA using Agfa ortho film (25 ASA) under 100× magnification.

3. Results and discussion

Fig. 1 shows the Fourier transform infrared (FT-IR) spectrum of $PPY^+(NO_3^-)$ membrane prepared electrochemically and washed thoroughly with de-ionized water after removal from the electrolytic cell. The observed prominent vibrational bands and their assignments are given in Table 1. In general, it is difficult to characterize anion bands due to overlapping of strong absorptions of oxidized polymers and solvents [13(a)]. The low absorption bands at 680 and 613 cm^{-1} are due to C–H and N–H out of plane bending of pyrrole moiety in $PPY^+(NO_3^-)$, respectively [13(b)]. The bands due to C=C and C=N stretching at 1547 and 1185 cm^{-1}, respectively, in $PPY^+(NO_3^-)$ arise due to vibrational mode of respective bonds of oxidized pyrrole moiety. The broad bands at 1309 and 1380 cm^{-1} arise due to mixed bending and stretching vibrations associated with C–N bond of oxidized pyrrole ring and N–O bond of nitrate (NO_3^-) moiety, respectively [13(c)]. The bands at 1475, 1042 and 794 cm^{-1} arise due to C–C stretching vibration, C–H deformation and C–H wagging vibrations, respectively. Fig. 2(a) shows the three-dimensional surface topography of $PPY^+(NO_3^-)$ membrane. From AFM analysis, we found that the surface roughness of this membrane to be $\sim 0.1 \pm 0.01$ nm. It also revealed that the polymer membranes were homogeneous with respect to the surface roughness (Fig. 2(a)). It is worthwhile to mention here that the surface roughness ($\sim 0.1 \pm 0.01$ nm) of $PPY^+(NO_3^-)$ membrane is best suited for the seeding and proliferation of human endothelial cell. Scanning electron micrograph (Fig. 2(b)) of the polymer membrane shows a morphology akin to cauliflower

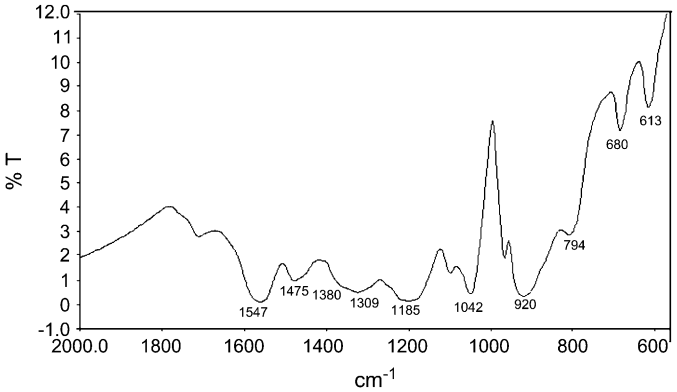

Fig. 1. FT-IR spectrum of $PPY^+(NO_3^-)$ composite membrane.

Table 1
Band assignment of FT-IR spectrum of $PPY^+(NO_3^-)$ membrane

Sr. no.	Band assignment	Wave number (cm^{-1})
1	C=C (pyrrole ring) vibrational mode	1547
2	C–C	1475
3	N–O	1380
4	C–N (stretching mode)	1309
5	C=N	1185
6	C–H (deformation)	1042
7	C–H (wagging)	794
8	C–H (out of plane bending)	680
9	N–H (out of plane bending)	613

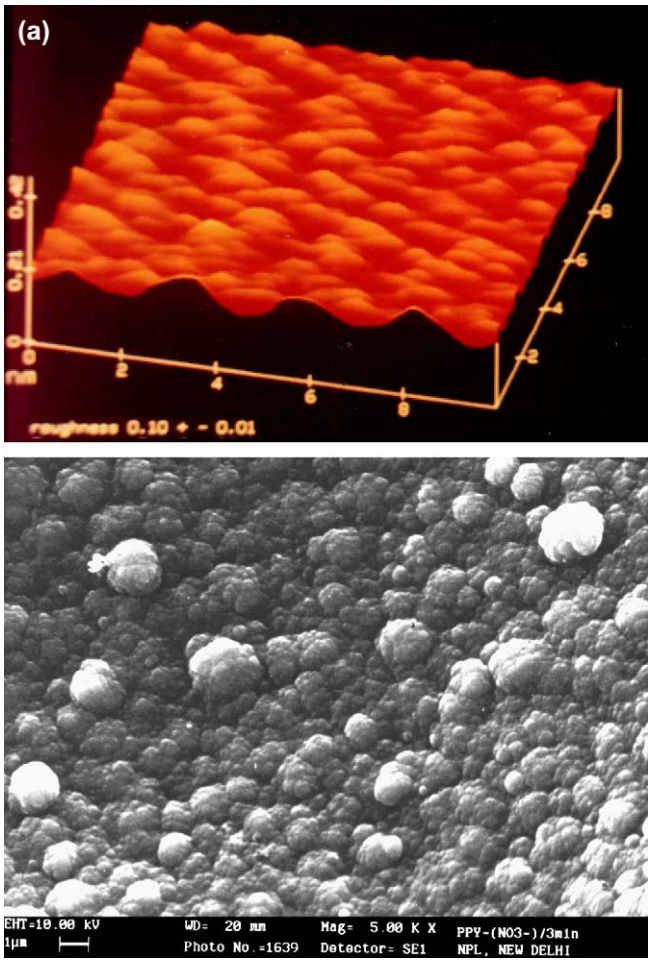

Fig. 2. (a) AFM surface topographs, (b) SEM surface micrographs of $PPY^{+}(NO_3^{-})$ composite membrane.

as reported earlier [14]. The morphology was found to be quite uniform and dense. Thus, the physical character of the $PPY^{+}(NO_3^{-})$ surface was akin to and well suited for cell attachment as reported earlier in the case of polypyrrole–heparin and ethylene–vinyl alcohol copolymers [15,16].

Fig. 3 shows the variation of measured dc conductivity (σ_{dc}) as functions of (a) $1000/T$, (b) $T^{-1/2}$, (c) $T^{-1/3}$ and (d) $T^{-1/4}$ in the temperature range 13–300 K for $PPY^{+}(NO_3^{-})$ film. The room temperature dc conductivity (σ_{dc}) and activation energy (E_A) of $PPY^{+}(NO_3^{-})$ film were $\sim$10 S/cm and $\sim$0.029 eV, respectively. Conductivity was found to decrease with the decrease in the temperature (Fig. 3(a)) as it has been observed in many other conjugated polymers [3,17,18]. It is evident from this figure that the temperature dependence of σ_{dc} does not follow an Arrhenius-type of behavior. Such a behavior of σ_{dc} is generally believed to be associated with the localized nature of the charge carriers in conjugated polymers as visualized by Mott's variable range hopping (VRH) model [19]. In this case, the variation of electrical conductivity as a function of temperature can be described by this formula:

$$\sigma_{dc} = \sigma_0 \exp\left\{-\left(\frac{T_0}{T}\right)^n\right\} \quad (1)$$

where the exponent n is connected with the dimensionality. Here, n is 1/2 for one-dimensional, 1/3 for two-dimensional and 1/4 for three-dimensional variable range hopping transport. For three-dimensional variable range hopping (3D-VRH) transport, T_0 and σ_0 are given [3,19–21] as

$$T_0 = \frac{\lambda\alpha^3}{k_B N(E_F)} \quad (2)$$

and

$$\sigma_0 = e^2 R^2 \nu_{ph} \times N(E_F) \quad (3)$$

where

$$R = \left\{\frac{9}{8\pi\alpha k_B T \times N(E_F)}\right\}^{1/4} \quad (4)$$

Here T_0 is the characteristic temperature, σ_0 is the conductivity at infinite temperature, e is the electronic charge, ν_{ph} is the phonon frequency ($\sim 10^{13}$ Hz), R is the average hopping distance between the two sites and λ is the dimensionless constant and is assumed to have a value $\sim$18.1 [3]. $\alpha(=1/r_p)$ is the coefficient of exponential decay of the localized states involved in the hopping process whereas k_B is the Boltzmann's constant and $N(E_F)$ is the density of states at the Fermi level. The average hopping energy W is given by

$$W = \frac{3}{4\pi R^3 \times N(E_F)} \quad (5)$$

The temperature dependence of dc conductivity as a function of $T^{-1/2}$, $T^{-1/3}$ and $T^{-1/4}$ (Fig. 3(b–d)) demonstrates that the $\log \sigma_{dc}$ versus $T^{-1/4}$ plot, corresponding to the 3D-VRH transport as suggested by Mott [19], gives most linear behavior ($\sim$0.99942 – see Fig. 3(d)) over the whole temperature range of investigation. Therefore, it is envisaged that the hopping conduction of $T^{-1/4}$ type may dominate the electrical transport mechanism in $PPY^{+}(NO_3^{-})$ films and, accordingly, different Mott's parameters have been evaluated by using Eqs. (2)–(5). The value of T_0 has been estimated from Fig. 3(d) and found to be $\sim 1.05 \times 10^5$ K. The calculated values of $N(E_F)$, R and W are $\sim 7.41 \times 10^{22}$ cm^{-3} eV^{-1}, 4.866×10^{-8} cm and 0.028 eV, respectively, obtained after assuming a reasonable value [20] of $\alpha^{-1} = 3$ Å. The magnitude of the value of $N(E_F)$ is consistent with the values obtained earlier for other conjugated polymers [3,17,18,20,21].

The activation energy (E_A), evaluated from $\log \sigma_{dc}$ versus $1000/T$ plot (Fig. 3(a)), is shown as a function of temperature in Fig. 4(a). The temperature dependent activation energy [21] shows that the band conduction model is inadequate to explain the conductivity of $PPY^{+}(NO_3^{-})$ films. The plot of $\log E_A$ versus $\log T$ (Fig. 4(b)) represents a straight line. From the slope of this straight line, we have estimated the value of n to be 1/4. The temperature dependent activation energy (Fig. 4(a)) suggests that the variable range hopping can also be qualitatively explained if hopping of polarons is considered. It has been suggested [21,22] that for an ordered material having

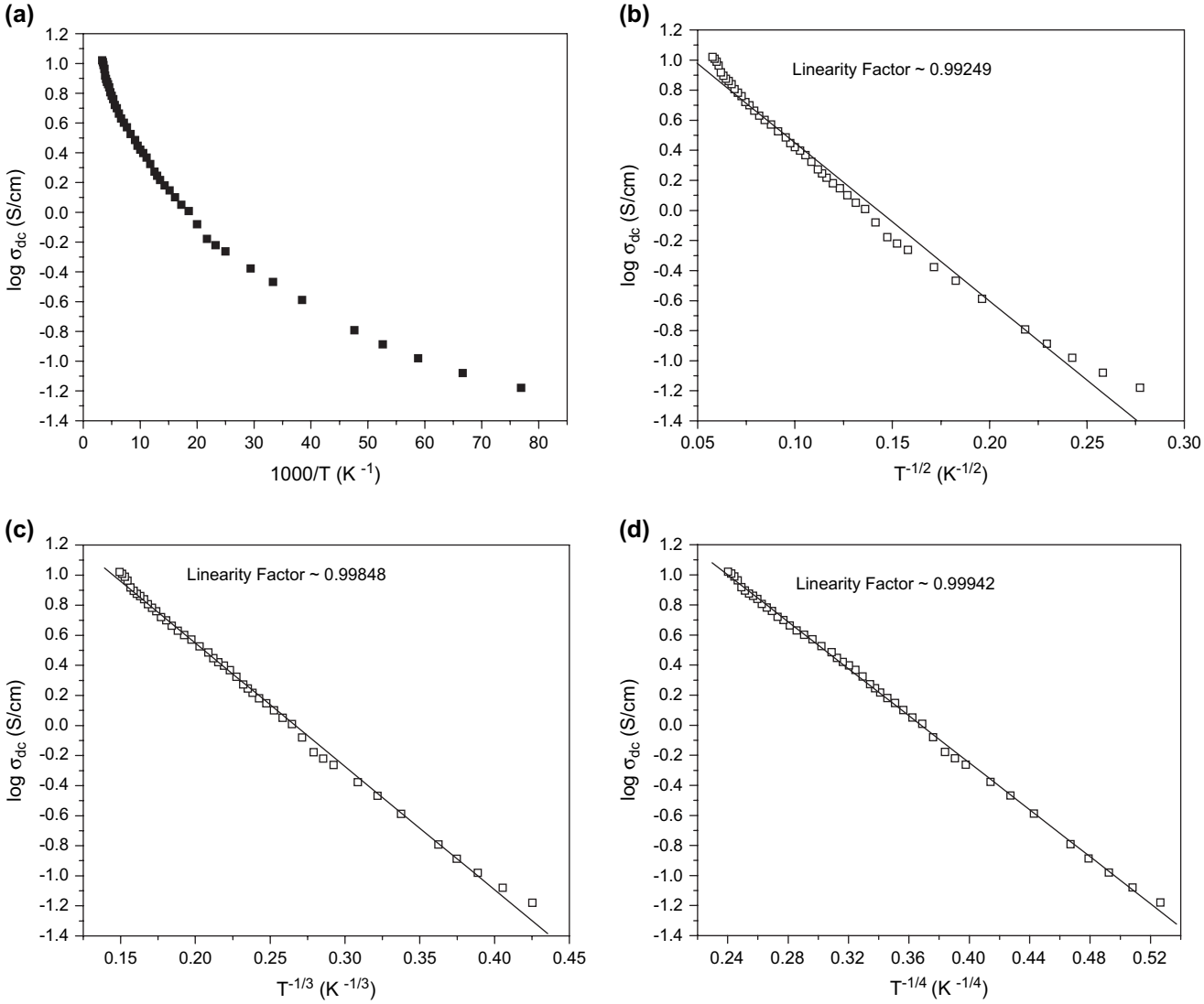

Fig. 3. Plots of $\log \sigma_{dc}$ as functions of (a) $1000/T$, (b) $T^{-1/2}$, (c) $T^{-1/3}$ and (d) $T^{-1/4}$ in the temperature range 13–300 K.

polaronic conduction the multi-phonon processes are gradually replaced at lower temperatures by the processes in which the only contribution to the jump frequency of the polaron is due to single optical phonon absorption and emission. The variation of activation energy for such a process is given [21,22] by

$$E'_A = E_A \left\{ \frac{\tanh(\hbar\omega_0/4k_BT)}{(\hbar\omega_0/4k_BT)} \right\} \quad (6)$$

where $\hbar = h/2\pi$, $\omega_0 = 2\pi\nu_{ph}$, E_A is the room temperature activation energy evaluated from Fig. 3(a) and E'_A is the activation energy calculated at different temperatures using Eq. (6). The theoretical plot of the right hand side of Eq. (6) is shown by a solid line in Fig. 4(a) assuming the characteristic phonon frequency $\nu_{ph} \sim 10^{13}$ Hz. The polaronic hopping conduction can give a temperature-independent activation energy where the multi-phonon process dominates. However, the temperature dependent activation energy (Fig. 4(a)) rules out the above possibility confirming the applicability of Mott's 3D-VRH conduction mechanism in this system. Therefore, we may conclude that the 3D-VRH conduction dominates the electrical transport mechanism in $PPY^+(NO_3^-)$ films confirming the validity of the analysis carried out by using Mott's VRH theory [19].

Studies were carried out to see the seeding and proliferation of endothelial cells on $PPY^+(NO_3^-)$ membranes which showed sign of apoptosis within 24 h of seeding these cells on the membranes (Fig. 5(a)). This is evident by the presence of apoptotic bodies around many cells and they maintained their round shape similar to post trypsinized state. They were also sluggish in sticking to the surface and in attaining their normal multi-polar shape. However, after 24 h, 20–25% of the cells started adhering to the membrane surface and in 48–72 h they attained their usual multi-polar shape and started dividing (Fig. 5(b)). At different points on the surface, a clump of cells was divided and grew horizontally and vertically in 72–96 h. We did not grow these cells beyond 96 h. However, these

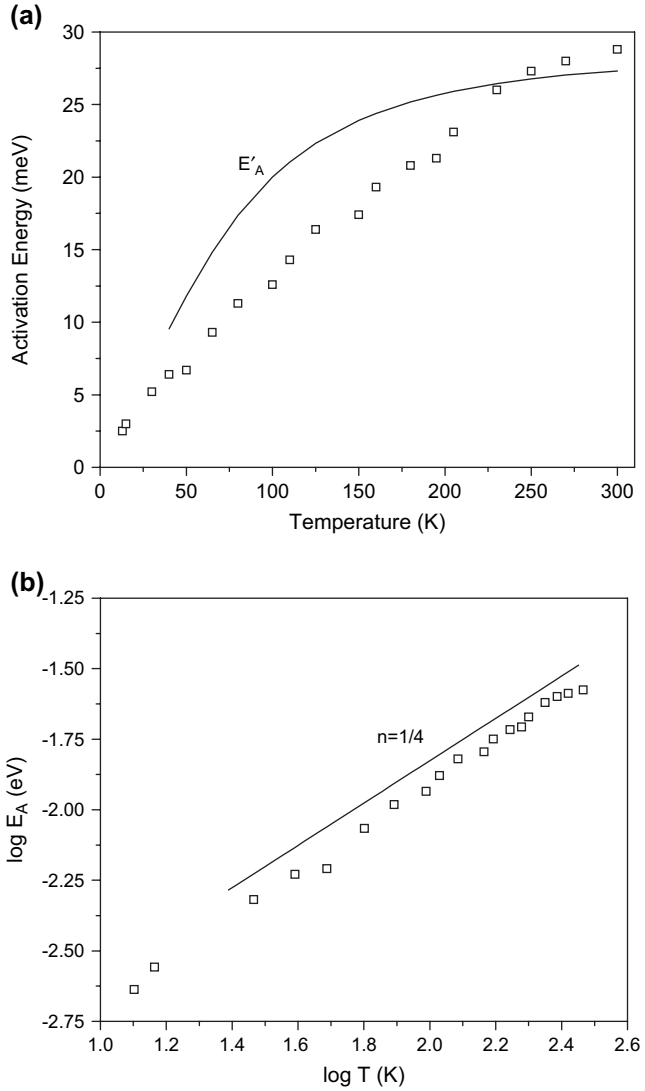

Fig. 4. (a) Activation energy (E_A) derived from Fig. 3(a) plotted as a function of temperature in the range 13–300 K. The solid line shows the calculated activation energy E'_A using Eq. (6) and (b) the plot of $\log E_A$ versus $\log T$ in the temperature range 13–300 K. The solid line corresponds to $T^{-1/4}$, slope $n = 1/4$.

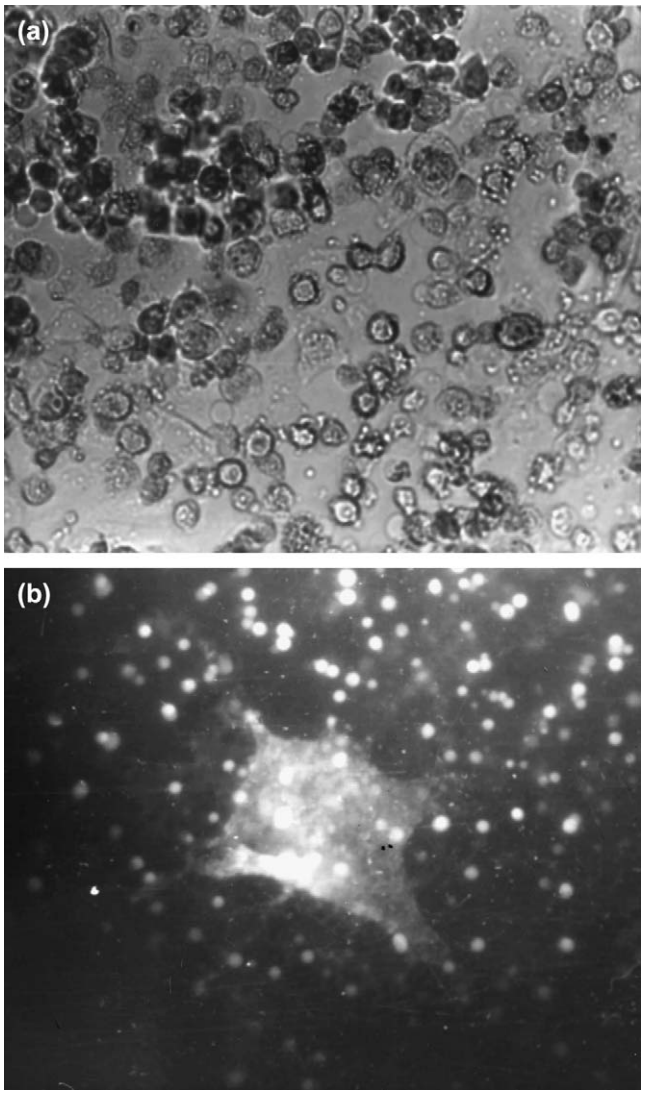

Fig. 5. (a) Human endothelial cells seeded on polypyrrole/sodium nitrate composite membrane and (b) proliferation of human endothelial cells seeded on polypyrrole/sodium nitrate composite membrane after 72 h (the photographs were taken under 100× magnification).

observations prove that the endothelial cells can be grown on the surface of these membranes for a longer period of time to achieve full confluency. Furthermore, a monolayer cell culture is possible by improving culture technique and applying some adhesive on the surface of these $PPY^+(NO_3^-)$ membranes.

4. Conclusions

The electrical transport mechanism in $PPY^+(NO_3^-)$ membranes can be described by Mott's 3D-VRH model. The physical feature of the $PPY^+(NO_3^-)$ surface was found to be well suited for the cell attachment and subsequent growth and development. These observations indicate that the human endothelial cells could be grown successfully on the surface of $PPY^+(NO_3^-)$ membranes which may find potential application in biocompatible organ development program.

Acknowledgements

The authors are thankful to Director, National Physical Laboratory, New Delhi for his interest in this work and to Mr. Rajiv K. Singh, Mr. S.B. Samanta, Mr. K.N. Sood all of NPL, New Delhi for their help. Thanks are also due to Dr. Ramesh C. Juyal, NII, New Delhi, for extending photographic facilities.

References

[1] Skotheim TA, Elsenbaumer RL, Reynolds JR. Handbook of conducting polymers. New York: Marcel Dekker; 1998.
[2] Rodriguez J, Grande HJ, Otero TF. Handbook of organic conductive molecules and polymers. In: Nalwa HS, editor. Chichester: Wiley; 1997. p. 415.
[3] Singh R, Narula AK. J Appl Phys 1997;82:4362–71.

[4] Anderson JM, Defife K, Mcnally A, Collier T, Jenney C. J Mater Sci Mater Med 1999;10:579–88.
[5] Petillo O, Margarucci S, Peluso G, Barbarisi A, Melone MAB, Ambosio L, et al. J Mater Sci Mater Med 1999;10:595–600.
[6] Aoki T, Tanino M, Sanui K, Ogata N, Kumakura K. Biomaterials 1996;17:1971–4.
[7] Williams RL, Doherty PJ. J Mater Sci Mater Med 1994;5:429–33.
[8] Wong JY, Langer R, Inngber DE. Proc Natl Acad Sci USA 1994;91:3201–4.
[9] Saoudi B, Jammul N, Anbel ML, Chehimi MM, Dodin G. Synth Met 1997;87:97–103.
[10] Quan DP, Lewis TW, Wallace GG, Viet PH. Anal Sci 2001;17 (Suppl.):i745–8.
[11] Schmidt CE, Shastri VR, Vacanti JP, Langer R. Proc Natl Acad Sci USA 1997;94:8948–53.
[12] Collier JH, Camp JP, Hundson TW, Schmidt CE. J Biomed Mater Res 2000;50:574–84.
[13] (a) Kato H, Nishikawa O, Matsui T, Honma S, Kakado H. J Phys Chem 1991;95:6011–4; Kato H, Nishikawa O, Matsui T, Honma S, Kakado H. J Phys Chem 1991;95:6014–6;
(b) Street GB, Clarke TC, Krounbi M, Kanazawa K, Lee V, Pfluger P, et al. Mol Cryst Liq Cryst 1982;83:253;
(c) Tian B, Zerbi G. J Chem Phys 1990;92:3886–91; Tian B, Zerbi G. J Chem Phys 1990;92:3892–8; Qian R, Qiu J, Shen D. Synth Met 1987;18:13–8.
[14] Singh R, Narula AK, Tandon RP, Rao SUM, Panwar VS, Mansingh A, et al. Synth Met 1996;79:1–6.
[15] Garner B, Hodgson AJ, Wallace GG, Underwood PA. J Mater Sci Mater Med 1999;10:19–27.
[16] Delguerra RS, Cascone MG, Ricci D, Martinoia S, Parodi MT, Ahluwalia A, et al. J Mater Sci Mater Med 1996;7:8–17.
[17] Singh R, Arora V, Tandon RP, Mansingh A, Chandra S. Synth Met 1999;104:137–44.
[18] Singh R, Kaur A, Yadav KL, Bhattacharya D. Curr Appl Phys 2003;3:235–8.
[19] Mott NF, Davis EA. Electronic processes in non-crystalline materials. London: Oxford University Press; 1979.
[20] Maddison DS, Tansley TL. J Appl Phys 1992;72:4677–82.
[21] Singh R, Narula AK, Tandon RP, Mansingh A, Chandra S. J Appl Phys 1996;79:1476–80.
[22] Holstein T. Ann Phys 1959;8:343–89.